Reactions of Laser-Ablated Boron Atoms with Ethylene and Ethane. Infrared Spectra and DFT Calculations for Several Novel BC_2H_x (x = 1, 2, 3, 4, 5) Molecules

Lester Andrews,* Dominick V. Lanzisera,‡ and Parviz Hassanzadeh†

University of Virginia, Department of Chemistry, Charlottesville, Virginia 22901

Yacine Hannachi

Lab. de Physico-Chimie Moleculaire (CNRS UMR 5803), Universite Bordeaux I, F-33405 Talence Cedex, France

Received: December 5, 1997; In Final Form: March 2, 1998

Laser-ablated boron atoms have been reacted with ethylene during condensation in excess argon. The BC_2H_3 closed-shell isomers borirene $(CH)_2BH$, ethynylborane H_2BCCH, and borallene $HBCCH_2$ have been identified from infrared spectra by using ^{10}B, ^{13}C, and D substitution and BP86/6-311G* isotopic frequency calculations. The observation of both cyclic aromatic and aliphatic products suggests that the reaction proceeds through both exothermic C═C addition and C−H insertion reaction mechanisms. Evidence is presented for the most stable BC_2H_4 radicals, namely, cyclic $\overline{BHCHCH_2}$ and aliphatic H_2BCCH_2, which require H-atom migration within the intermediates first formed. Ethane gave a smaller yield of the same products, including linear HBCC and BCCH, vinylborane $H_2BC_2H_3$, and an enhanced yield of the C−C insertion product $CH_3B{=}CH_2$.

Introduction

Reactions of laser-ablated boron atoms with ethylene have been studied for three reasons: (1) to prepare the smallest aromatic molecule, borirene, $(CH)_2BH$, (2) to form the borirane radical, BC_2H_4, analogous to the borirene radical produced by the addition of B atoms to C_2H_2, and (3) to compare isotopic frequencies calculated by density functional theory (DFT) with observed values in order to support the identification of new BC_2H_x species.

The aromatic $(CH)_2BH$ molecule has been examined by quantum chemical calculations[1−5] but has so far escaped experimental detection, although substituted borirenes have been prepared.[6,7] Previous work in this laboratory has shown that cold boron atoms add to C_2H_2 to form the cyclic borirene BC_2H_2 radical,[8,9] and the analogous reaction to form the cyclic borirane BC_2H_4 radical is suggested although H-atom rearrangement in the BC_2H_4 radical is expected to be easier than for BC_2H_2. Likewise, substituted boriranes have been prepared experimentally,[10,11] but the simple borirane radical BC_2H_4 and borirane BC_2H_5 species have only been studied theoretically.[12−17]

Finally, laser-ablated boron atoms are quite reactive and a large number of product molecules have been prepared in this laboratory. In such complicated chemical systems as the previous B + C_2H_2, B + CH_4 and B + NH_3 investigations,[8,9,18,19] comparison between quantum chemical calculated and observed vibrational frequencies of isotopic product molecules proved essential for the identification of new product molecules, and such is also the case for the present B + C_2H_4 system.

Experimental Section

The apparatus for pulsed-laser ablation of boron, matrix isolation, and FTIR spectroscopy has been described previously.[8,9,18−20] Mixtures of (0.50 and 0.25%) C_2H_4, C_2H_6, C_3H_8 (Matheson), $^{13}C_2H_4$, C_2D_2, CH_2CD_2, and C_2D_6 (MSD Isotopes) in Ar were co-deposited at 3 mmol/h for 2−4 h onto a 10 ± 1 K cesium iodide window along with boron atoms. The fundamental 1064-nm beam of a Nd:YAG laser (Spectra Physics DCR-11) operating at 10 Hz and focused with a fl = +10 cm lens ablated the target using a 20−30 mJ per 10 ns pulse. Two samples of boron were employed: natural boron ^{n}B (Aldrich, 80.4% ^{11}B, 19.6% ^{10}B) and ^{10}B (Eagle Pitcher Industries, 93.8% ^{10}B, 6.2% ^{11}B). Following deposition, a Nicolet 750 or 60SXB Fourier transform infrared (FTIR) spectrometer collected infrared spectra from 4000 to 400 cm^{-1} using a liquid nitrogen cooled MCT detector. The spectral resolution was 0.5 cm^{-1} with an accuracy of ±0.2 cm^{-1}. After sample deposition, broadband mercury arc photolysis (Philips 175 W, 240−580 nm) produced changes in the FTIR spectra. Annealing to 25, 30, 35, and 40 K, with photolysis both before and after the first annealing, also increased or decreased some of the spectral features.

Density functional theory (DFT) calculations were performed on potential product molecules using the Gaussian 94 program package.[21] All calculations used the BP86 functional[22] and the 6-311G* basis sets,[23,24] because this functional works well in predicting experimental frequencies and isotopic shifts for small first-row compounds.[25] A complete theoretical study will include comparisons with the hybrid B3LYP functional and QCISD calculations, which will be reported separately.[26]

Results

The FTIR spectra of samples prepared by reacting laser-ablated boron atoms with ethylene, ethane, and propane in excess argon and DFT calculations on possible reaction products will be presented.

B + C_2H_4. Reactions were done for both natural and ^{10}B-enriched boron atoms, and infrared spectra were examined for

† Present address: National Institute of Standards and Technology, Gaithersburg, MD.

‡ Present address: Instruments SA, Horiba Group, Edison, NJ.

S1089-5639(98)00437-X CCC: $15.00
Published on Web 04/17/1998

TABLE 1: Product Absorptions (cm^{-1}) Observed in the Reaction of Boron Atoms (^{10}B and ^{11}B) with Isotopic Ethylene Molecules ($^{12}C_2H_4$, $^{13}C_2H_4$, and $^{12}C_2D_4$)

10−12−1	11−12−1	10−13−1	11−13−1	10−12−2	11−12−2	identification
609.4	609.4	604.6	604.6	478.2	478.0	?
736.6	736.6	734.8	734.8	542.4	542.4	C_2H_2
639.2	637.6	633.3	631.8	536.6	530.4	LB8
653.7	653.0	652.3	651.6	482.7	481.6	borirene (**1**)
826.9	826.5	819.3	819.2	652.3	650.9	LB10
843.4	832.5	833.9	823.5			borirene (**1**)
855.5	847.7	850.0	841.9			LB10
875.9	864.3	868.6	857.6	652.3	650.9	LB8
1045.6	1031.3	1030.7	1013.2			$H_2BC_2H_3$
1177.6	1169.5	1152.9	1144.6			borirene (**1**)
1197.0	1170.6	1172.2	1147.7	1196.0	1169.4	BC_2H_2 (E)
1200.7	1175.3	1178.6	1154.4	1145.4	1126.0	borirene (**1**)
1226.0	1213.9	1224.6	1212.6			$H_2BC_2H_3$
1256.7	1248.0	1250.5	1243.1	926.6	958.3	?
1292	1261	1285	1250	1328	1293	$(CH_3)_2B$?
1348.5	1347.1	1342.8	1341.5			LB10
1416.1	1414.1		1402.2			$H_2BC_2H_3$
				828.9	814.1	H_2BCCH (**2**)
				1020.6	997.4	H_2BCCH (**2**)
1538.8	1536.8	1488.8	1487.9	1472	1472.5	$H_2BC_2H_3$
1641.7	1613.7	1628.2	1598.5			?
1677.2	1631.2	1656.4		1640.0		$CH_3B{=}CH_2$
1700.0	1660.5	1681.5	1643.0	1658.8	1607.7	$(CH_2BCH_2)^-$
1772.5	1770.6			1732.5	1732.1	LB10
1861.0	1821.9	1861.0	1821.9	1861.0	1821.9	HBO
1870.7	1859.8	1812.9	1800.9	1776.0	1774.6	$HBCCH_2$ (**3**)
1907	1854	1907	1854.5	1907	1854.5	BO
2002.5	1995.3	1935.1	1926.9	1908.1	1907.7	HBCC (**A**)
2041.7	2039.2	1971.0	1968.1	1923.0	1918.8	BCCH (**B**)
2054.0	2054.0	2035.9	2035.9			C_xH_y (**X**)
2060.5	2058.1	1990	1988.1	1842.9	1832.5	H_2BCCH (**2**)
2084.1	2080.4	2013.9	2010.4			HBCCH (**C**)
2268.3	2259.4	2268.3	2259.4	1696.3	1682.8	$(H_2)BH$
2306.9	2298.3	2306.9	2298.3	1721.7	1709.4	BH
2517.6	2510.5	2515.5	2507.7	1883.4	1868.2	?
2534.5	2520.5	2532.6	2519.4	1851.7	1842.4	$C_2H_5BH_2$?
2547.7	2537.6	2546.9	2537.2	1943.9	1937.5	?
2570.9	2556.4	2570.5	2556.1			?
2583.3	2568.7	2591.0		1953.0	1933.5	LB10
2584.6	2570.2	2584.7	2570.4			$H_2BC_2H_3$
2601.4	2587.7	2601.4	2587.7			BH_3
2607.8	2593.3	2607.5	2592.6	1966.4	1945.9	H_2BCCH (**2**)
2635.4	2621.6	2634.7	2621.3	1982.8	1962.2	LB8
2656.4	2639.6	2659.2	2643.6	2029.9	2006.1	borirene (**1**)
2663.3	2651.2	2663.1	2650.7			$(C_2H)(BH)$
	2669.5	2634.9				borirene (**1**)
2742.7	2724.6					$HB{=}CH_2$
2773.8	2757.7	2772.3	2756.0	2185.0	2168.2	$HBCCH_2$ (**3**)
2780.2	2763.2	2779.0	2762.0	2173.0		HBCC (**A**)

new absorptions with boron isotopic shifts. Such bands appeared as 1:4 doublets for ^{10}B and ^{11}B absorptions using natural boron (marked in figures) and only the ^{10}B absorption was observed with the enriched sample. Traces of boron oxides and HBO from oxide contamination on the target surface were observed.[20] In addition BH, $(H_2)BH$, BH_3, C_2H, C_2H_2, and C_2H_3 were evidenced by weak absorptions in these experiments.[9,27−29] One new product at 2054.0 cm^{-1} (labeled X), also common to Be experiments with C_2H_4 but not C_2H_6, is probably due to a hydrocarbon fragment that cannot be identified here.

Infrared spectra recorded on the Nicolet 750 instrument had better signal-to-noise than those recorded earlier on the Nicolet 60 spectrometer, and the former are illustrated in the figures. Table 1 lists the isotopic frequencies for the new product absorptions observed here. Bands are grouped by photolysis and stepwise annealing behavior. Figure 1 shows the B−H stretching region for $^{10}B + {}^{12}C_2H_4$, $^{n}B + {}^{12}C_2H_4$, and $^{n}B + {}^{13}C_2H_4$ and Figures 2 and 3 compare spectra in the 2100−1920 and 920−600 cm^{-1} regions for the same samples. Bands labeled **A**, **B**, **C**, and **D** have been identified in previous C_2H_2 work[9] and bands noted LB refer to BC_2H_4 structural isomers first calculated by Largo and Barrientos.[17] The numbers **1**, **2**, and **3** indicate the new BC_2H_3 product isomers formed here. Isotopic spectra in the BC_2 ring stretching region have been illustrated in a preliminary communication on borirene.[30] The strongest new band in this system is shown in Figure 3 at 637.6 cm^{-1} (labeled LB8) along with C_2H_2 produced in the co-deposition reaction. One investigation done with a mixture of $^{12}C_2H_4$ and $^{13}C_2H_4$ gave the sum of pure isotopic spectra, indicating that only one ethylene molecule is involved in the major processes.

B + C_2D_4. Both boron isotopic reactions were done with C_2D_4 at different concentrations, and the spectra are shown in Figure 4 for the 2040−1660 cm^{-1} region. Photolysis and annealing behavior matched most bands with the hydrogen counterparts as listed in Table 1. One experiment with a mixture of C_2H_4 and C_2D_4 gave the sum of pure isotopic spectra. The two boron isotopic samples were reacted with CH_2CD_2, and

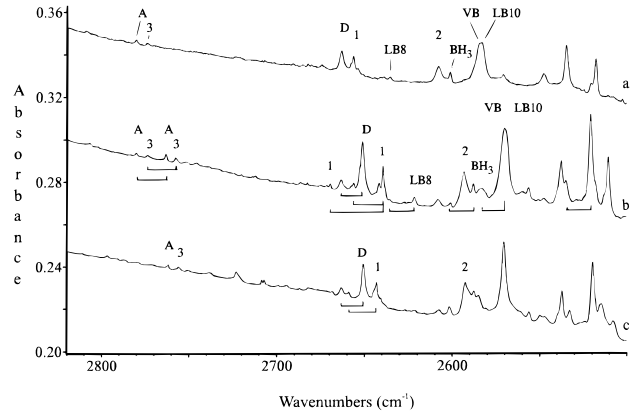

Figure 1. Infrared spectra in the 2820−2500 cm^{-1} region for laser-ablated boron atoms co-deposited with argon/ethylene = 200/1 samples on a CsI window at 10 ± 1 K. (a) $^{10}B + {}^{12}C_2H_4$, (b) $^{n}B + {}^{12}C_2H_4$, and (c) $^{n}B + {}^{13}C_2H_4$.

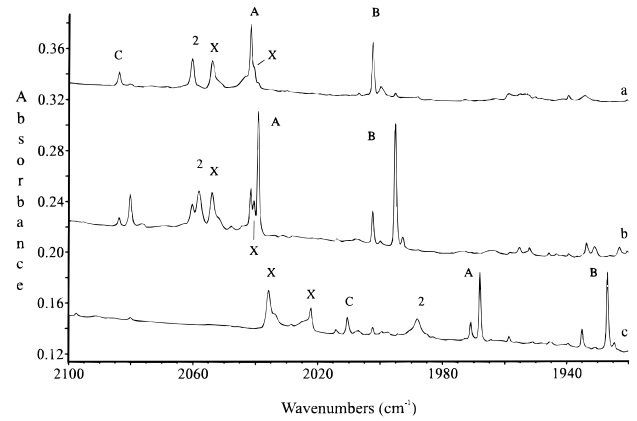

Figure 2. Infrared spectra in the 2100−1920 cm^{-1} region for laser-ablated boron atoms co-deposited with argon/ethylene = 200/1 samples on a CsI window at 10 ± 1 K. (a) $^{10}B + {}^{12}C_2H_4$, (b) $^{n}B + {}^{12}C_2H_4$, and (c) $^{n}B + {}^{13}C_2H_4$. Bands labeled X are due to hydrocarbon fragment.

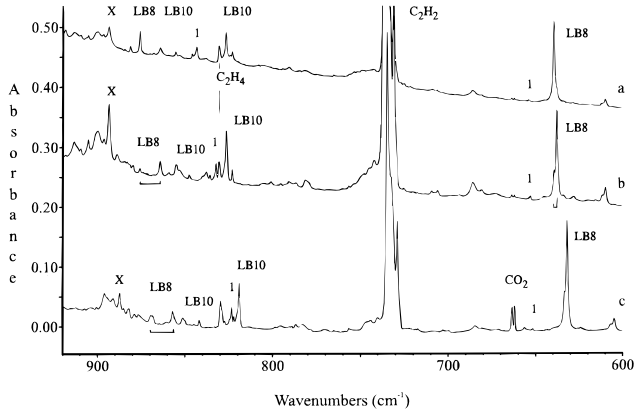

Figure 3. Infrared spectra in the 920−600 cm^{-1} region for laser-ablated boron atoms co-deposited with argon/ethylene = 200/1 samples on a CsI window at 10 ± 1 K. (a) $^{10}B + {}^{12}C_2H_4$, (b) $^{n}B + {}^{12}C_2H_4$, and (c) $^{n}B + {}^{13}C_2H_4$. Band labeled X is due to hydrocarbon fragment.

both species **A** (HBCC, DBCC) and **B** (BCCH, BCCD)[9] were observed (^{10}B and ^{11}B) with a slight preference for the deuterated species.

B + C_2H_6 and C_2D_6. Similar experiments were done with ^{n}B and ^{10}B and ethane-h_6 and -d_6 samples in argon, and the same major product bands were observed with reduced (one-quarter to one-sixth) intensity compared to ethylene along with weak ethylene and acetylene "product" absorptions. The major exception is the 1677.2, 1631.2 cm^{-1} 1:4 natural boron isotopic doublet, which was only slightly weaker in C_2H_6 compared to C_2H_4 experiments. A new band was observed at 2597.0 cm^{-1} (^{n}B) and 2611.7 cm^{-1} (^{10}B), and this was comparable to the strongest absorption in the B−H stretching region. A new weak 1:4 doublet observed at 1217.1/1212.8 cm^{-1} showed substantial growth on photolysis. One experiment was done with ^{11}B (97.5%) and the ^{10}B components from the ^{n}B experiments were, of course, absent.

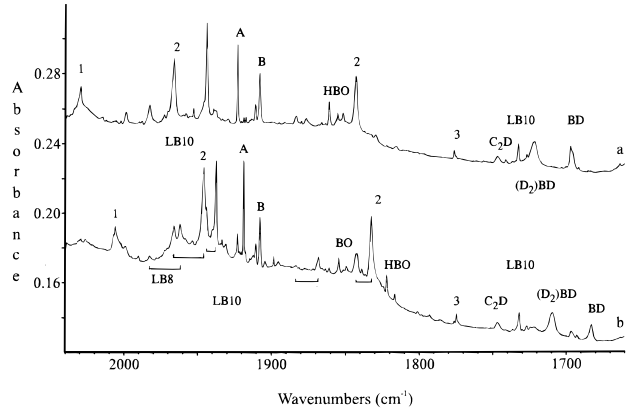

Figure 4. Infrared spectra in the 2040−1660 cm^{-1} region for laser-ablated boron atoms co-deposited with Ar/C_2D_4 = 200/1 samples on a CsI window at 10 ± 1 K. (a) ^{10}B and (b) ^{n}B.

TABLE 2: Isotopic Frequencies (cm^{-1}) Calculated for Linear HBCC and BCCH at the DFT/BP86/6-311G* Level

		HBCC[a]			
1−11−12−12	141.4	738.9	1137.7	2005.2	2800.6
intensity[b]	0	14 × 2	4	556	51
1−10−12−12	141.8	747.5	1164.5	2012.4	2819.0
1−11−13−13	136.8	737.3	1118.0	1935.6	2799.6
2−11−12−12	134.0	594.1	1093.6	1907.0	2197.2
		BCCH[a]			
11−12−12−1	86.7	688.7	877.1	2059.5	3353.5
intensity[b]	3 × 2	34 × 2	191	266	14
10−12−12−1	87.5	688.7	906.2	2060.9	3353.5
11−13−13−1	84.3	681.9	866.9	1986.4	3335.6
11−12−12−2	82.5	545.9	867.1	1924.9	2602.8

[a] Bond lengths, left-to-right, for HBCC are 1.179, 1.376, and 1.291 Å and for BCCH are 1.538, 1.227, and 1.076 Å. HBCC is more stable than BCCH by 15.3 kcal/mol. [b] Intensities (km/mol) are given for the top, most abundant isotopic molecule.

B + C_3H_8. Both boron samples were co-deposited with propane in argon. Methane, acetylene, and ethylene were observed as products (major bands $A = 0.15-0.20$), but ethane was not observed. The **A**, **B**, and **C** product bands were detected. The 1175.3 and 2639.6 cm^{-1} bands were observed ($A = 0.005$) for species **1**, the 2058.1 and 2593.3 cm^{-1} bands for species **2**, and the 1859.8 cm^{-1} band for species **3** ($A = 0.003$). In addition weak 637.6, 864.3, 826.5, and 2570 cm^{-1} bands were observed with the same relative intensities as before. The only product band observed in the 1600 cm^{-1} region with ^{n}B was at 1656.7 cm^{-1} ($A = 0.002$) with a ^{10}B counterpart at 1697.0 cm^{-1}.

Calculations. Calculations were first done by using BP86/6-311G* for the closed-shell isomers HBCC and BCCH investigated earlier at the MP2 level.[9] Here the former is lower in energy by 15 kcal/mol than the latter and the strongest absorption is predicted 10 cm^{-1} higher for the former and 20 cm^{-1} higher for the latter in contrast to 52 cm^{-1} higher for the former and 35 cm^{-1} lower for the latter at the MP2 level.[9] Clearly the BP86 calculation does a better job at predicting

SCHEME 1

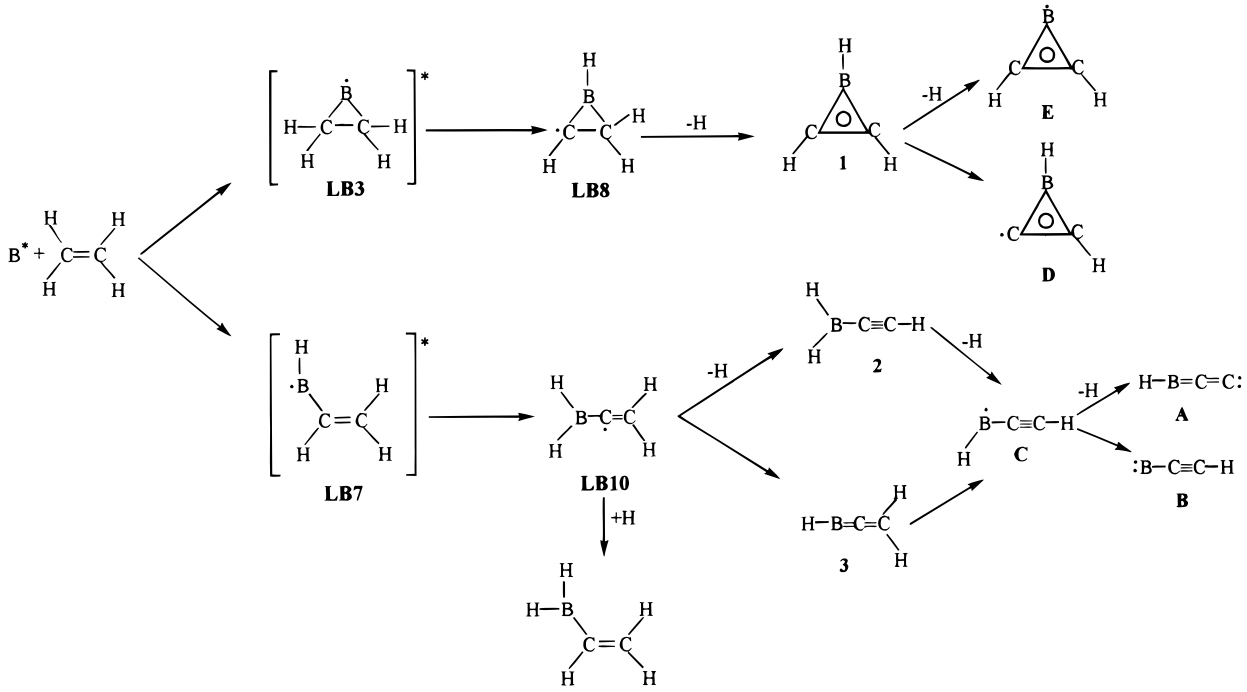

TABLE 3: Frequencies (cm^{-1}) Calculated for the Planar C_{2v} Isomers $(CH)_2BH$, H_2BCCH, and $HBCCH_2$ at the DFT/BP86/6-311G* Level

$(CH)_2BH$[a]	B_1	B_2	B_1	A_1	B_2	A_2	B_2	A_1	A_1	A_1	B_2	A_1
$(12-1)_2-11-1$	642.1	761.9	842.5	869.9	875.2	985.4	1157.9	1179.2	1500.9	2668.2	3095.1	3120.7
intensity,[b] km/mol	15	4	54	11	24	0	15	45	0	82	23	8
$(12-1)_2-10-1$	643.0	762.4	852.1	871.3	887.5	985.4	1166.8	1205.4	1508.1	2683.3	3095.1	3121.0
H_2BCCH[c]	B_1	B_2	B_2	B_1	B_2	A_1	B_1	A_1	A_1	A_1	B_2	A_1
$1-11-12-12-1$	252.5	288.1	543.9	730.6	847.4	905.2	955.3	1177.6	2071.8	2519.5	2595.0	3371.8
intensity,[b] km/mol	4	2	64	30	15	22	53	41	63	101	99	28
$1-10-12-12-1$	253.1	288.4	543.9	730.6	855.9	923.0	968.2	1191.3	2073.2	2525.7	2610.1	3371.8
$1-11-13-13-1$	245.4	280.6	539.6	723.3	842.5	894.0	954.3	1176.9	1998.0	2519.4	2595.0	3354.2
$2-11-13-13-2$	227.4	248.9	425.5	581.8	694.9	754.3	772.2	985.7	1823.1	1942.2	1949.1	2611.4
$HBCCH_2$[d]	B_2	B_1	B_2	B_1	B_1	B_2	A_1	A_1	A_1	A_1	A_1	B_2
$1-11-12-12-1_2$	252.6	263.4	541.5	768.9	965.9	1031.3	1080.4	1448.5	1892.6	2784.3	2972.8	3029.2
intensity,[b] km/mol	11	7	8	30	31	0.1	3	1	113	36	54	19
$1-10-12-12-1_2$	254.5	264.1	546.1	778.5	965.9	1031.3	1103.3	1450.4	1902.9	2802.4	2972.8	3029.2
$1-11-13-13-1_2$	246.4	256.4	541.4	766.5	955.6	1019.3	1065.2	1441.1	1831.0	2783.5	2967.2	3017.0
$2-11-12-12-2_2$	228.2	233.4	416.7	628.9	733.8	826.6	928.9	1155.5	1789.3	2140.0	2193.6	2254.5

[a] Bond lengths: B−C = 1.482, C−C = 1.360, B−H = 1.190, C−H = 1.093 Å. Angles: C−B−C = 54.6°, C−C−B = 62.7°. [b] Intensities for top, most abundant isotopic molecule. [c] Bond lengths: B−H = 1.203, B−C = 1.503, C−C = 1.224, C−H = 1.074 Å. Angles: H−B−H = 120.1°, B−C−C = C−C−H = 180.0°. [d] Bond lengths: B−H = 1.179, B−C = 1.366, C−C = 1.328, C−H = 1.102 Å. Angles: H−C−H = 115.0°, H−B−C = B−C−C = 180.0°.

experimental frequencies for these molecules although the relative energies may not be as accurate. Isotopic shifts are also well-described by DFT as shown in Table 2. A similar calculation for the open-shell HBCCH molecule gave frequencies in better agreement with observed values than previous MP2 but poorer agreement than earlier QCISD calculations.[9]

Next BP86 calculations were done for cyclic planar borirene $(CH)_2BH$, and frequencies are listed in Table 3 for boron isotopic molecules. The frequencies and isotopic shifts compare favorably with those calculated at the QCISD level.[26] The aliphatic isomers were also investigated; the planar C_{2v} molecules H_2BCCH and $HBCCH_2$ were found to be 11 and 23 kcal/mol, respectively, above borirene. Similar relative energies were determined at the B3LYP and QCISD levels.[26] Calculated frequencies for isotopic substitution at all atomic positions are also given in Table 3.

Largo and Barrientos (hereafter LB) investigated 10 structures of formula BC_2H_4 at the HF and MP4 levels and predicted their relative energies.[17] The five most stable of these structures (LB number 3, 7, 8, 9, 10) have been reoptimized at the BP86/6-311G* level, and frequencies for four isotopic molecules of the most stable ring and open isomers analogous to LB8 and LB10 are given in Table 4. The $\overline{BHCHCH_2}$ isomer calculated here is 11 kcal/mol more stable than borirene radical and *does not* have a plane of symmetry; the ring bond lengths are slightly longer than those of LB (Table 4). The H_2BCCH_2 isomer calculated here is 23 kcal/mol more stable than borirene radical and *does not* have a symmetry plane (dihedral angles, Table 4); the bond lengths are similar to those of LB10.

Another isomer with boron in the central position, H_2CBCH_2, is found to be the global minimum (4 kcal/mol below H_2BCCH_2) with D_2 symmetry, B−C (1.434 Å), C−H (1.096 Å), angle H−C−H (122.8°), and dihedral angle (142.8°). The strongest band calculated at 1307 cm^{-1} and the diagnostic antisymmetric C−B−C stretching mode, 1487 cm^{-1}, were not observed here.

TABLE 4: Isotopic Frequencies (cm^{-1}) Calculated at the DFT/BP86/6-311G* Level for the $\overline{BHCHCH_2}$ and H_2BCCH_2 Isomers

$\overline{BHCHCH_2}$[a]	frequencies														
1−11−12	376	530	637	710	785	832	888	968	1108	1308	1407	2687	2910	2990	3132
intensity[b]	34	5	53	16	19	23	18	8	1	10	5	49	7	22	4
1−10−12	383	531	639	713	789	839	889	974	1109	1327	1413	2701	2910	2990	3132
1−11−13	371	529	632	707	782	828	880	954	1082	1290	1398	2686	2904	2980	3121
2−11−12	327	388	495	538	609	672	707	773	974	1069	1247	2017	2114	2215	2329
H_2BCCH_2[c]	frequencies														
1−11−12	264	298	371	768	800.4	858	885	892	1138	1348	1772	2498	2567	2993	3049
intensity[b]	1	2	1	19	55	21	3	3	11	14	12	63	82	0	0
1−10−12	265	299	371	773	801.3	869	894	901	1150	1349	1776	2504	2582	2993	3049
1−11−13	258	291	371	764	791.2	857	874	880	1137	1342	1708	2498	2567	2987	3037
2−11−12	226	258	263	602	647.4	702	722	744	904	1046	1721	1830	1920	2193	2264

[a] C_1 symmetry; bond lengths: B−CH_2 = 1.655, B−CH = 1.438, C−C = 1.468, B−H = 1.188, C−H = 1.091, C−H_2 = 1.102, 1.107 Å. Angles: C−B−C = 56.1, C−CH_2−B = 54.4°, H−C−H = 111.2°, C−B−H = 161.4°, B−C−H = 146.6°. Dihedral angles: H−C−B−CH_2 = 131.0°, H−C−B−H = −61.5°. [b] Intensities (km/mol) given for the top, most abundant isotopic molecule. [c] C_2 symmetry; bond lengths: B−C = 1.483, C−C = 1.307, B−H = 1.205, C−H = 1.100 Å. Angles: B−C−C = 180.0°, H−B−H = 120.2, H−C−H = 115.7°, C−C−H = 122.2°, C−B−H = 120.0°. Dihedral angles: H−BCC−H = 67.7 and −112.4°.

TABLE 5: Isotopic Frequencies (cm^{-1}) Calculated for $H_2BC_2H_3$ and CH_3BCH_2 at the DFT/BP86/6-311G* Level

isotopes	$H_2BC_2H_3$[a] frequencies																	
1−11−12	197	360	532	815	919	981	988	1022	1081	1201	1287	1413	1600	2495	2570	3026	3037	3114
intensity[b]	0.5	0.3	2	9	18	23	63	21	4	37	2	53	48	125	147	29	16	22
1−10−12	197	363	532	823	930	986	996	1022	1085	1213	1288	1415	1601	2501	2585	3026	3037	3114
1−11−13	195	355	530	814	909	974	983	1018	1070	1200	1271	1399	1554	2495	2570	3019	3028	3102
2−11−12	149	295	392	625	742	744	785	820	833	940	1013	1143	1528	1817	1925	2205	2246	2319
isotopes	CH_3BCH_2[c] frequencies																	
1−11−12	101	257	301	569	619	779	889	895	1280	1310	1411	1433	1638	2939	2997	3020	3055	3116
intensity[b]	2	1	0	3	99	4	45	5	21	3	10	9	191	1	12	6	7	0
1−10−12	101	261	309	570	619	781	901	901	1283	1310	1411	1434	1688	2939	2997	3020	3055	3116
1−11−13	101	257	299	565	614	758	880	888	1277	1300	1409	1431	1616	2935	2987	3009	3049	3104
2−11−12	72	205	266	442	486	678	726	777	945	1014	1023	1062	1603	2117	2210	2236	2238	2310

[a] Bond lengths: B−C = 1.542, C−C = 1.355, B−H = 1.208, 1.206, C−H = 1.100, C−H_2 = 1.097, 1.096 Å. Angles: H−B−H = 119.2°, B−C−C = 121.2, H−C−C = 117.3, H−C−H = 116.1°. [b] Intensities (km/mol) given for the top, most abundant isotopic molecule. [c] Bond lengths: C−H_3 = 1.108, 1.103, C−B = 1.531, B=C = 1.390, C−H_2 = 1.096 Å. Angles: C−B−C = 178.3°, C−H_2 = 114.4°, C−H_3 = 106−109°.

The anions $(CH_2BCH_2)^-$ and $(BH_2CCH_2)^-$ were calculated, and although the former neutral was more stable, the latter anion was lower by 2 kcal/mol. The $(CH_2BCH_2)^-$ anion has D_{2d} symmetry, B−C (1.435 Å) and C−H (1.103 Å) bond lengths and angle H−C−H (123.5°). The antisymmetric C−B−C stretching mode was calculated at 1660.5 cm^{-1}.

Closed-shell species of formula BC_2H_5 including vinylborane $H_2BC_2H_3$ have been considered by several groups.[13,31,32] The planar $H_2BC_2H_3$ molecule was calculated with DFT; the C=C bond is 0.02 Å longer than calculated for C_2H_4 and the B−C length 1.54 Å is appropriate for a single bond. The isomer $CH_3B{=}CH_2$ is more stable by 0.2 kcal/mol at this level of theory, but vinylborane is more stable at other levels.[13,26] The $B{=}CH_2$ double bond is 0.005 Å longer than in $HB{=}CH_2$ calculated at the same BP86/6-311G* level. The cyclic borirane isomer is 14 kcal/mol higher. The fourth isomer $HB{=}CHCH_3$ is less stable by 16 kcal/mol. Table 5 presents isotopic frequencies for the two most stable BC_2H_5 isomers which are observed in these experiments.

Finally, calculations were done for the series CH_3BH_2, $(CH_3)_2B$, $(CH_3)_2BH$, and $(CH_3)_3B$, and the results are summarized in Table 6 giving selected infrared absorptions.

Discussion

The new product absorptions will be identified with the assistance of isotopic shifts at all atomic positions and BP86/6-311G* frequency calculations. Reaction mechanisms will be proposed; to make the discussion easier to follow, the mechanism for the boron−ethylene reaction is now presented in Scheme 1 to help identify the product molecules.

A(HBCC) and B(BCCH). The linear HBCC and BCCH molecules were major products in the C_2H_2 reaction with atomic boron,[9] and the same absorptions have been observed here with the same relative intensities and half the relative yield as with the C_2H_2 reaction investigated again under the same experimental conditions. Improved sensitivity has enabled observation of the weak B−H stretching mode of HBCC at 2763.2 cm^{-1} and isotopic counterparts given in Table 1. The DFT calculations predict this band at 2800.6 cm^{-1} with a ^{10}B shift of 18.4 cm^{-1} (observed 17.0 cm^{-1}) and a ^{13}C shift of 1.0 cm^{-1} (observed 1.2 cm^{-1}).

C(HBCCH), D((C$_2$H)(BH)), and E((CH)$_2$B). Weak infrared bands were observed for these open and cyclic C_2H_2 reaction products as listed in Table 1. They are mentioned here because of involvement in the overall reaction mechanism.

(CH)$_2$BH. Three stable products of formula BC_2H_3 were observed and identified in part because of the excellent fit of DFT frequency calculations and the high confidence in these calculations for closed-shell molecules. The small aromatic ring borirene molecule has been characterized in a preliminary communication from five fundamental vibrations of six isotopic molecules.[30] The diagnostic B−C_2 ring stretching vibration at

TABLE 6: Selected Infrared Absorptions in the B−C Stretching Region Calculated for Methylborane Isotopic Species at the DFT/BP86/6-311G* Level[a]

CH_3BH_2	∠H−B−C = 121.0°, 1.557 Å, 1.102−1.115 Å, 1.208 Å
1−11−12	1051.2 (62), 1300.4 (78), 2560.0 (158)
1−10−12	1065.4, 1304.2, 2574.8
1−11−13	1047.9, 1288.3, 2560.0
2−11−13	1047.9, 1288.3, 2560.0
2−11−12	859.7 (4), 1027.0 (24), 1916.6 (96)
$(CH_3)_2BH$	∠C−B−C = 125.3°, 1.567 Å, 1.102−1.108 Å, 1215 Å
1−11−12	987.2 (50), 1302.0 (195), 1433.2 (1)
1−10−12	1004.6, 1308.3, 1436.8
1−11−13	980.4, 1288.9, 1429.6
2−11−12	860.8 (32), 1210.3 (188), 1008.3 (49)
$(CH_3)_2B$	∠C−B−C = 130.2°, 1.553 Å, 1.102−1.111 Å
1−11−12	1142.1 (38), 1306.7 (127), 1397.1 (9)
1−10−12	1171.5, 1315.5, 1399.4
1−11−13	1138.1, 1290.6, 1395.0
2−11−12	1058.3 (3), 1214.9 (131), 1026.3 (23)
$(CH_3)_3B$	∠C−B−C = 120.0°, 1.581 Å, 1.103−1.111 Å
1−11−12	667.3 (4), 1143.2 (69 × 2), 1305.8 (121 × 2)
1−10−12	667.8, 1172.9, 1311.0
2−11−12	587.9 (0), 1187.0 (149 × 2), 1026.0 (21 × 2)
2−10−12	588.2, 1217.8, 1026.2

[a]Frequencies, cm^{-1} (infrared intensities, km/mol). Bond lengths: B−C, C−H, and B−H, respectively.

1175.3 cm^{-1} for borirene $(CH)_2{}^{11}BH$ is nearly the same (1170.6 cm^{-1}) for the borirene radical $(CH)_2B$ but the H→D shift for the former (to 1126.0 cm^{-1}) is much more than for the latter (to 1147.7 cm^{-1}).[8] Note that the $B-C_2$ ring stretching vibration in $(CH)_2BH$ is nearly the same as in cyclic-BC_2 itself (1194.6 cm^{-1}).[33,34] An average scale factor (0.9965) times the DFT calculated isotopic frequencies for this mode predicts the 11−12, 10−12, 11−13, 10−13 isotopic frequencies to ±0.4 cm^{-1} and $(CD)_2BD$ to ±1.0 cm^{-1} for both ^{10}B and ^{11}B.

The stronger B−H stretching mode was also observed and this band is labeled 1 in Figure 1. The Fermi resonance between this fundamental and the sum of symmetric $B-C_2$ and C═C ring stretching modes, which results in a *blue* ^{13}C shift, has been discussed.[30] This Fermi resonance is stronger for the $(^{12}CH)_2{}^{11}BH$ and $(^{13}CH)_2{}^{10}BH$ isotopic molecules and these combination bands are observed at 2669.5 cm^{-1} (Figure 1b) and at 2634.9 cm^{-1}.

Two other modes were observed at 1169.5 and 653.0 cm^{-1} for the natural isotopic molecule. Although the DFT frequency calculations are 11 cm^{-1} lower than both the observed values, the isotopic shifts are predicted to ±1 cm^{-1}. Calculations at the QCISD level predict these bands at 1198 and 657 cm^{-1} with correct isotopic shifts.[26]

The final borirene band is an out-of-plane deformation mode observed at 832.5 cm^{-1} and calculated at 842.5 cm^{-1}. Although this harmonic calculation predicts the ^{10}B shift (9.6 cm^{-1}) just short of the observed (10.9 cm^{-1}) value, the observed ^{13}C shift (10.0 cm^{-1}) is underestimated (3.8 cm^{-1}). The calculated H/D ratio (1.217) denotes substantial anharmonicity in this out-of-plane deformation mode and suggests quartic character of the type observed for CH_3 and CH_2X radicals.[35] It should be noted that other absorptions for borirene could be observable, but many of the spectral regions are congested and bands may be masked by other product and very intense unreacted precursor absorptions.

H_2BCCH. The aliphatic H_2BCCH isomer is only 10.4 kcal/mol higher than the aromatic ring isomer, and the DFT calculations predict two strong $B-H_2$ stretching modes at 2595.0, 2519.5 cm^{-1} and a strong C≡C stretching mode at 2071.8 cm^{-1}. The 2593.3 and 2058.1 cm^{-1} bands (labeled 2) increase 10% on photolysis and decrease 5% on 25 K and 40% on 35 K annealing and exhibit 1:4 doublets with natural isotopic boron, verifying the participation of a single boron atom in these vibrational modes. Of even more importance, the DFT calculations predict the $^{10}B-^{11}B$ and $^{12}C-^{13}C$ isotopic shifts for these modes to be 15.1, 2.4 and 0.0, 73.8 cm^{-1}, respectively, and the observed shifts are 14.5, 2.4 and 0.3, 70.0 cm^{-1}. The boron isotopic shift shows that the 2593.3 cm^{-1} band is due to the antisymmetric $B-H_2$ stretching mode. Although the symmetric stretch is predicted to have comparable intensity, no bands are observed with the appropriate isotopic shift and photolysis behavior. The D_2BCCD molecule is more complicated because these modes now fall in the same region, but again DFT calculations predict two observed modes within 12 cm^{-1} of the observed values.

It is interesting to note that the C≡C stretching modes for H_2BCCH (2058.1 cm^{-1}), HBCCH (2080.4 cm^{-1}), and BCCH (2039.2 cm^{-1})[9] are in near agreement. Their large $^{12}C-^{13}C$ shifts (70.0, 70.0, 71.1 cm^{-1}) and small $^{10}B-^{11}B$ shifts (2.4, 3.7, 2.5 cm^{-1}) verify the almost pure C≡C character of this vibrational mode, which is observed at 1973.8 cm^{-1} in the Raman spectrum of acetylene.[36]

$HBCCH_2$. The other aliphatic $HBCCH_2$ isomer is 22.8 kcal/mol above the aromatic ring isomer, and from the observed spectrum of HBCC at 2763.2 and 1995.3 cm^{-1}, the $HBCCH_2$ molecule is expected to have bands in these regions. DFT predictions of strong bands at 2784.3 and 1892.6 cm^{-1} are in very good agreement with sharp bands observed at 2757.7 cm^{-1} (labeled 3) and at 1859.8 cm^{-1} that show 16.5, 10.9 and 1.8, 58.9 cm^{-1} $^{10}B-^{11}B$ and $^{12}C-^{13}C$ isotopic shifts compared to DFT predicted 18.1, 10.3 and 0.8, 61.6 cm^{-1} shifts, respectively. These bands also show the 1:4 natural boron isotopic doublets required for a single boron atom vibration. Again deuterium substitution is the acid test because of increased mode mixing, and observed bands at 2168.2 and 1774.6 cm^{-1} are in very good agreement with 2193.6 and 1789.3 cm^{-1} calculated bands. The correct DFT description of mode mixing is found in comparison of the observed and calculated $^{10}B-^{11}B$ isotopic frequency shifts (Table 3).

BC_2H_4 Products. The experimental observation and theoretical characterization of three closed-shell BC_2H_3 isomers in the B + C_2H_4 reaction systems suggests that some BC_2H_4 radical intermediate species may also be trapped in these matrix isolation experiments. Although DFT frequency calculations are expected to be less accurate for these radical species, some clear guidance for the identification of two BC_2H_4 product molecules is provided here.

The most stable C_{2v} cyclic BC_2H_4 addition product, the borirane radical, is 40 kcal/mol below B + C_2H_4 and is predicted to have strong absorptions in the 950 and 880 cm^{-1} regions.[16] Although the former is masked by C_2H_4 absorption, no band with appropriate isotopic shifts is observed in the latter region. However, the migration of one H to B gives a cyclic species that is another 11 kcal/mol lower at the BP86 level of theory, namely, $\overline{BHCHCH_2}$. Our DFT frequency calculations (Table 4) predict a very strong band at 637.1 cm^{-1} for this isomer,

with +1.7 and −4.8 cm^{-1} ^{10}B and ^{13}C shifts, respectively, which is in very good agreement with the strongest product band observed here (637.6 cm^{-1} for natural isotopes with 639.2 cm^{-1} ^{10}B and 631.8 cm^{-1} ^{13}C counterparts, labeled LB8, Figure 3). The prediction of two other strong bands at 831.7 and 2686.5 cm^{-1} with isotopic shifts in agreement with the observed 864.3 and 2621.6 cm^{-1} bands supports the present identification of the rearranged borirane radical $\overline{BHCHCH_2}$. It is important to note that the 864.3 and 637.6 cm^{-1} (^{11}B) and the 875.9 and 639.2 cm^{-1} (^{10}B) bands track precisely on photolysis and 25 and 35 K annealing (better than ±5% integrated areas). Although the 864.3 cm^{-1} band by itself could be due to the borirane radical, the 637.6 cm^{-1} band cannot, and taken together this species that grows on annealing is not the borirane radical but its more stable rearrangement isomer $\overline{BHCHCH_2}$. The 637.6 cm^{-1} band is unique and of many attempts only $\overline{BHCHCH_2}$ has been able to model this band and its isotopic counterparts.

The insertion of B into a C−H bond gives HBC_2H_3; this planar radical (LB7) is a saddle point but 59 kcal/mol more stable than B + C_2H_4 at the MP4 level.[17] At the DFT/BP86 level, this radical has the H bonded to B out of the C_2H_3 plane, all real frequencies, but only one infrared band with reasonable calculated intensity. The B−H stretching mode is predicted at 2725 cm^{-1} (22 km/mol), which is even higher than the B−H mode for borirene (2668 cm^{-1}). We see no additional product absorption in this region and, on this basis, conclude that the initial insertion HBC_2H_3 radical is not trapped here. There are bands in the B−H stretching region that cannot be assigned, such as 2510.5 cm^{-1}, but this band is probably too low for HBC_2H_3.

We have no evidence for the higher-energy open structure corresponding to LB9. The 1536.8 and 1213.9 cm^{-1} bands that increase 10% on photolysis and decrease slightly on annealing do not have the boron and carbon isotopic shifts calculated by DFT for LB9, but on the other hand, an excellent fit is found for the closed-shell vinylborane $H_2BC_2H_3$ molecule formed by H-atom addition to LB10.

The more stable BC_2H_4 species, LB10, has the H_2BCCH_2 structure. The strongest unique band is calculated at 800.4 cm^{-1} with +0.9 cm^{-1} ^{10}B, −9.2 cm^{-1} ^{13}C, and −153 cm^{-1} D shifts, which are in reasonable agreement with the sharp 826.5 cm^{-1} absorption that decreases 10% on photolysis and decreases on annealing and has +0.3, −7.6, and −175.6 cm^{-1} shifts, respectively. A similar 1347.1 cm^{-1} band also decreases 10% on photolysis and has a calculated position at 1347.6 cm^{-1} with predicted +1.7 cm^{-1} ^{10}B and −5.1 cm^{-1} ^{13}C shifts as compared to the observed +1.4 cm^{-1} and −5.6 cm^{-1} shifts, respectively. The C═C stretch is calculated at 1772.4 cm^{-1} with a +2.5 cm^{-1} ^{10}B shift. A sharp 1770.6 cm^{-1} band with a ^{10}B counterpart at 1772.5 cm^{-1} has matching photolysis and annealing behavior. The $^{13}C_2H_4$ experiments had lower yield and did not reveal this band, but the C_2D_4 experiments gave bands at 1732.5 and 1732.1 cm^{-1} for ^{10}B and ^{11}B, which are close to the more intense calculated 1720.8 and 1720.5 cm^{-1} values.

The strongest band calculated for LB10 is the antisymmetric B−H_2 stretching mode at 2567.3 cm^{-1} with a +14.8 cm^{-1} calculated ^{10}B shift. The split 2570.2, 2568.7 cm^{-1} band decreases at 2568.7 cm^{-1} on photolysis as does the lower half of the 2584.5, 2583.3 cm^{-1} band with ^{10}B. These bands show a small positive ^{13}C shift, which is again indicative of Fermi resonance probably with the C═C stretching mode. The most likely band to combine with the C═C stretching mode and exhibit Fermi resonance with the antisymmetric B−H_2 stretching mode is the antisymmetric B−H_2 rocking mode calculated at 858.5 cm^{-1}. A weak band with matching isotopic and photolysis behavior is observed at 847.7 cm^{-1}. The sum 1770.6 + 847.7 = 2618.3 cm^{-1} clearly falls above 2568.7 cm^{-1} and the projected ^{13}C counterpart at 2545 ± 5 cm^{-1} is below, and a positive ^{13}C shift on the B−H_2 stretching mode will result from this Fermi resonance interaction. In conclusion, the observation of five fundamentals with isotopic counterparts in very good agreement with DFT calculated isotopic frequencies strongly supports identification of this stable H_2BCCH_2 radical isomer.

BC_2H_5 Products. The 2570.2 cm^{-1} band in the B−H stretching region (labeled VB) shows the same photolysis and annealing behavior as the above-mentioned 1536.8 and 1213.9 cm^{-1} bands and weak 1414.1 and 1031.3 cm^{-1} bands. The closed-shell vinylborane molecule $H_2BC_2H_3$ was calculated to be stable (97 kcal/mol lower than LB10 + H atom) and the frequencies calculated for four isotopic molecules are given in Table 5. The calculated 2570, 1600, 1413, 1201, and 1031 cm^{-1} bands have isotopic counterparts in very good agreement with the observed bands. The C═C stretching mode at 1536.8 cm^{-1} is somewhat lower than the calculated value although the calculated value for C_2H_4 (1647 cm^{-1}) is also above the observed (1623 cm^{-1}) value.[36] The 1031.3 cm^{-1} band is primarily out-of-phase C−H_2 deformation and as such it interacts with the C−H and B−H_2 deformation modes, and the accurate calculation of this mode is difficult. As with other H_2B species observed here, the antisymmetric B−H_2 stretching mode is much stronger than the symmetric stretching mode despite the calculated intensity of the latter. Finally, we have not observed the complete spectrum of vinylborane, but the five assigned bands and isotopic shifts are in suficient agreement with calculations to support the identification of vinylborane.

The methyl-substituted compound $CH_3B{=}CH_2$ has one strong band calculated at 1687.9 cm^{-1} for ^{10}B with a large −50.0 cm^{-1} ^{11}B shift, −20.5 cm^{-1} ^{13}C shift, and a −36.5 cm^{-1} D shift. The observed 1677.2 cm^{-1} band shows a −46.0 cm^{-1} ^{11}B shift, a −20.8 cm^{-1} ^{13}C shift owing to the antisymmetric motion of B between two carbon atoms, and a −37.2 cm^{-1} deuterium shift. The same large boron isotopic shift has been observed for the isoelectronic $CH_3B{\equiv}NH$ molecule.[37] Similar DFT calculations predict $HB{=}CH_2$ at 1475 cm^{-1}, near the observed 1470 cm^{-1} value, and at 2759 cm^{-1}, near the 2725 cm^{-1} observed value,[18] and predict $HB{=}CHCH_3$ at 1552 and 2752 cm^{-1} (medium intensities). The failure to observe these latter bands indicates that only the more stable $CH_3B{=}CH_2$ isomer is observed here.

The other obvious BC_2H_5 product is borirane. This higher energy molecule like $HB{=}CHCH_3$ has one strong band, the B−H stretching mode, which is calculated at 2716 cm^{-1} by DFT. The only band in this region, a weak absorption at 2724.6 cm^{-1}, is due to $H_2C{=}BH$, a major product in the methane reactions.[18] Unfortunately, borirane was not observed in these experiments.

Other Absorptions. There remain other minor absorptions in this complicated chemical system that require special reactions. The characterization of a distinct C−B−C stretching mode in the stable $CH_3B{=}CH_2$ molecule demonstrates that boron insertion into the C═C bond can happen under proper circumstances. Two other observed bands have characteristic large boron isotopic shifts, the weak band at 1660.5 cm^{-1} and the broader band at 1261 cm^{-1}. The 1660.5 cm^{-1} band is due to the most photosensitive species produced here as the band is completely destroyed by photolysis and does not grow on annealing. The $(H_2CBCH_2)^-$ anion is isoelectronic with allene,

SCHEME 2

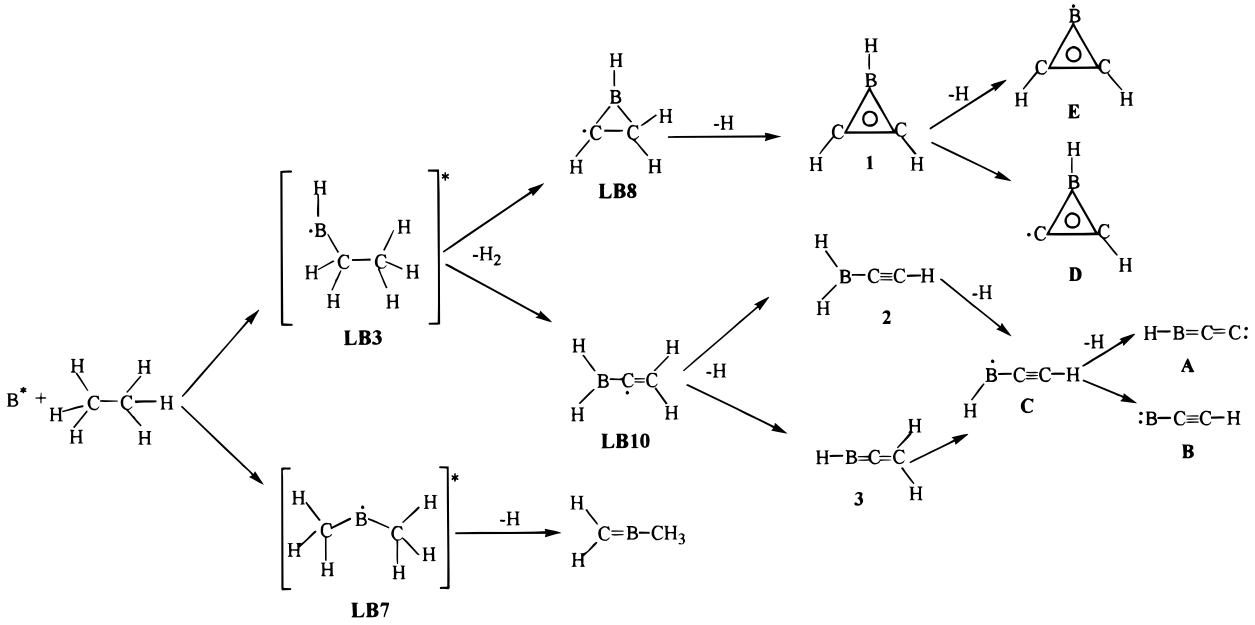

and the antisymmetric C−B−C stretching mode is the strongest infrared band (calculated at 1660.0 cm^{-1} (184 km/mol)). The calculated ^{10}B shift, +53.2 cm^{-1}, ^{13}C shift, −20.1 cm^{-1}, and D shift, −34.6 cm^{-1}, are compatible with the observed values although interaction with the out-of-phase terminal-CH_2 bending mode calculated at 1338 cm^{-1} has been *underestimated* by the DFT calculation. The 1660.5 cm^{-1} band is tentatively assigned to $(H_2CBCH_2)^-$ formed in the exothermic (−63 kcal/mol) electron capture reaction of the initial borirene radical intermediate. The presence of electrons in these laser ablation experiments has been shown in the observation of BO_2^-.[20]

The 1261 cm^{-1} band is in the region of the antisymmetric C−B stretching mode of trimethylboron (1155 cm^{-1}), with which it shares a large boron isotopic shift and a blue deuterium shift.[38] The 1261 cm^{-1} band grows on annealing (up to ×5), decreases on photolysis, and is slightly broader than most of the observed bands. The analogous CH_3BCH_3 radical can be produced here by H addition to vinylborane on annealing, and this tentative assignment is proposed for the 1261 cm^{-1} absorption. DFT calculations on this radical predict the strongest band at 1306.7 cm^{-1} but the isotopic shifts are not in good agreement. A higher level calculation of this large free radical is expected to give isotopic shifts in better agreement with the observed values.

The 2510.5, 2520.5, and 2537.6 cm^{-1} bands in the B−H stretching region remain to be identified. Observation of the H_2C-BH_2 species in methane experiments[18] at 2540.2 cm^{-1} (+14.6 cm^{-1} ^{10}B shift) strongly suggests that the 2520.5 cm^{-1} band (+14.0 ^{10}B shift) might be due to a similar $R-BH_2$ species. Our DFT calculations show that CH_3BH_2 absorbs in this spectral region, but the lack of other strong absorptions for CH_3BH_2 casts doubt on this assignment. The $C_2H_5BH_2$ species is a possibility. The 2510.5 cm^{-1} band is decreased by photolysis so a charged species cannot be ruled out.

Reaction Mechanisms. Boron atoms can react with ethylene to form the cyclic borirane radical (LB3) or the open vinylborane radical (LB7) as shown in Scheme 1. Borirane radical is 40 kcal/mol[16] more stable than B + C_2H_4 so the initial borirane radical BCH_2CH_2 formed contains excess internal energy, which can foster H-atom rearrangement to the more stable (−11 kcal/mol) cyclic radical $\overline{BHCHCH_2}$, the major species observed here. The failure to observe $\overline{BCH_2CH_2}$ suggests that the barrier to rearrangement to $\overline{BHCHCH_2}$ is considerably less than the overall reaction exothermicity. This is analogous to the formation of borirene radical BC_2H_2 from acetylene,[9] where in contrast to the present ethylene reaction, only some of the cyclic BC_2H_2 sustains H migration (to $\overline{BHCHC}$, species D). Hydrogen atom elimination from $\overline{BHCHCH_2}$ to form the stable aromatic borirene ring $\overline{BHCHCH}$ requires 33 kcal/mol and this energy is provided by the exothermic addition reaction. The elimination of another H-atom to form the radical species D and E requires excess energy in the initial boron atom reagent, and this extra energy is provided by the laser ablation process.[9,18]

Insertion into a C−H bond by B is exothermic by 59 kcal/mol and initiates another series of reactions leading to the lower energy allene-like H_2BCCH_2 radical species LB10 (−10 kcal/mol).[17] The significant reaction exothermicity helps to promote H-atom detachment (+55 and +68 kcal/mol, respectively, from DFT energies), giving the stable closed-shell aliphatic molecules H_2BCCH and $HBCCH_2$. Again with excess energy in the laser-ablated boron atom reagent, further H atom removal leads to the **A**, **B**, and **C** products of the B + C_2H_2 reaction.

Photolysis increases the more stable H_2BCCH isomer at the expense of $HBCCH_2$ or from the dissociation of H_2BCCH_2.

$$H-B{=}C{=}CH_2 \xrightarrow{h\nu} H_2B-C{\equiv}CH$$

$$H_2BCCH_2 \xrightarrow{h\nu} H_2B-C{\equiv}CH + H$$

The B atom reaction with CH_2CD_2 gave both **A** and **B** with deuterated counterparts slightly favored (by 20% in absorbance). Assuming that B atom insertion into C−H and C−D bonds proceeds at the same rate, it is clear that H is faster than D elimination, as expected (calculated intensities are less for the **D** species).

Reaction of B with C_2H_6 gave a relatively higher yield of $H_2C{=}BCH_3$ in addition to the products reported for C_2H_4 and C_2H_2, so another reaction mechanism must be available for B + C_2H_6, which is shown in Scheme 2. First, B insertion into

a C−H bond in C_2H_6 followed by H migration to boron and H elimination from terminal carbon gives vinylborane (VB) or followed by H_2 elimination can lead to all of the products shown in Scheme 1 as is observed in the ethane experiments. However, B insertion into the C−C bond gives a different radical, which can eliminate H to give the stable $H_2C{=}BCH_3$ molecule or CH_3 to give $H_2C{=}BH$. These bands *increase* on photolysis in ethane experiments. Note that these BC_2H_5 species can also be made from LB8 and LB10 by the addition of an extra H atom in processes that are exothermic by 119 and 96 kcal/mol, respectively.

The observation of BH and C_2H_2 as products of the ethylene reaction and BH, C_2H_2, and C_2H_4 as products of the ethane reaction show that another decomposition pathway for the initial insertion product is breaking of the newly formed B−C bond. The observation of C_2H, $(H_2)(BH)$, and BH_3 attests the production of H atoms and H_2 molecules in these reactions.

It is interesting to compare the addition vs insertion pathways for ethylene as determined by the relative yields of cyclic **1** and aliphatic **2** products with the relative yields of **1** and **2** using ethane. It is expected that the aliphatic species will be favored over the cyclic species with ethane and this is definitely the case. In fact, extra bands at 2611.7 cm^{-1} (^{10}B) and 2597.0 cm^{-1} (^{11}B) with ethane are probably due to a $(H_2)(H_2BCCH)$ complex.

Finally, some comment about the propane reaction products is in order. The major ethylene products LB8, LB10, **1**, **2**, **3**, **A**, **B**, and **C** were all observed with propane in substantially reduced yields as were C_2H_2, C_2H_4, and CH_4 bands. Clearly, boron insertion into a terminal C−H bond of propane followed by CH_4 elimination is equivalent to the top step in Scheme 2 using ethane with H_2 elimination. Weak bands at 1697.0 cm^{-1} (^{10}B) and 1656.7 cm^{-1} (^{11}B) with propane are probably due to the propane analogue of the bottom step in Scheme 2, namely, $H_2C{=}BC_2H_5$.

Conclusions

Laser-ablated boron atoms react with ethylene during condensation in excess argon to produce more than 12 novel BC_2H_x product molecules. The BC_2H_3 closed-shell isomers borirene $(CH)_2BH$, ethynylborane H_2BCCH, and borallene $HBCCH_2$ are identified from infrared spectra with ^{10}B, ^{13}C, and D substitution and BP86/6-311G* isotopic frequency calculations. The observation of both cyclic aromatic and aliphatic products suggests that the reaction proceeds through both C=C addition and C−H insertion mechanisms, which are exothermic reactions that can sustain further rearrangements in the products. Evidence is presented for the more stable cyclic $\overline{BHCHCH_2}$ and aliphatic H_2BCCH_2 radicals of BC_2H_4 stoichiometry. Ethane gives a smaller yield of the same products, including linear HBCC and BCCH, vinylborane $H_2BC_2H_3$, and the C−C insertion product $CH_3B{=}CH_2$. DFT calculations of vibrational frequencies for isotopic substitution at all atomic positions are clearly invaluable for the identification of novel BC_2H_x species.

Acknowledgment. This work was supported by the National Science Foundation and the Air Force Office of Scientific Research. The DFT calculations were done on the University of Virginia SP2 machine; we thank W. D. Bare for performing several calculations. Y. H. thanks IDRIS Project 970337 for computer time.

References and Notes

(1) Krogh-Jespersen, K.; Cremer, D.; Dill, J. D.; Pople, J. A.; Schleyer, P. v. R. *J. Am. Chem. Soc.* **1981**, *103*, 2589.
(2) Budzelaar, P. H. M.; Kos, A. J.; Clark, T.; Schleyer, P. v. R. *Organometallics* **1985**, *4*, 429.
(3) Budzelaar, P. H. M.; Kraka, E.; Cremer, D.; Schleyer, P. v. R. *J. Am. Chem. Soc.* **1986**, *108*, 561.
(4) Budzelaar, P. H. M.; van der Kerk, S. M.; Krogh-Jespersen, K.; Schleyer, P. v. R. *J. Am. Chem. Soc.* **1986**, *108*, 3960.
(5) Byun, Y.-G.; Saebo, S.; Pittman, C. U. *J. Am. Chem. Soc.* **1991**, *113*, 3689.
(6) Eisch, J. J.; Shafii, B.; Rheingold, A. L. *J. Am. Chem. Soc.* **1987**, *109*, 2526.
(7) Eisch, J. J.; Shafii, B.; Odom, J. D.; Rheingold, A. L. *J. Am. Chem. Soc.* **1990**, *112*, 81847.
(8) Martin, J. M. L.; Taylor, P. R.; Hassanzadeh, P.; Andrews, L. *J. Am. Chem. Soc.* **1993**, *115*, 2510.
(9) Andrews, L.; Hassanzadeh, P.; Martin, J. M. L.; Taylor, P. R. *J. Phys. Chem.* **1993**, *97*, 5839.
(10) Meyer, H.; Schmidt-Lukasch, G.; Baum, G.; Massa, W.; Berndt, A. *Z. Naturforsch. B* **1988**, *43*, 801.
(11) Wieczorek, C.; Allwohn, J.; Schmidt-Luckasch, G.; Hunold, R.; Massa, W.; Berndt, A. *Angew. Chem., Int. Ed. Engl.* **1990**, *29*, 389 and references therein.
(12) Budzelaar, P. H. M.; Krogh-Jespersen, K.; Clark, T.; Schleyer, P. von R. *J. Am. Chem. Soc.* **1985**, *107*, 2773 and references therein.
(13) Taylor, C. A.; Zerner, M. C.; Ramsey, B. *J. Organometallic Chem.* **1986**, *317*, 1.
(14) Liang, C.; Allen, L. C. *J. Am. Chem. Soc.* **1991**, *113*, 1878.
(15) Willerhausen, P.; Schmidt-Lukasch, G.; Kybart, C.; Allwohn, J.; Massa, W.; McKee, M. L.; Schleyer, P. von R.; Berndt, A. *Angew. Chem., Int. Ed. Engl.* **1992**, *31*, 1384.
(16) Hannachi, Y.; Hassanzadeh, P.; Andrews, L. *Chem. Phys. Lett.* **1996**, *250*, 421.
(17) Largo, A.; Barrientos, C. *Appl. Organomet. Chem.* **1996**, *10*, 283.
(18) Hassanzadeh, P.; Andrews, L. *J. Am. Chem. Soc.* **1992**, *114*, 9239. Hassanzadeh, P.; Hannachi, Y.; Andrews, L. *J. Phys. Chem.* **1993**, *97*, 6418. Hannachi, Y.; Hassanzadeh, P.; Andrews, L. *J. Phys. Chem.* **1994**, *98*, 6950.
(19) Thompson, C. A.; Andrews, L. *J. Am. Chem. Soc.* **1995**, *117*, 10 125. Thompson, C. A.; Andrews, L.; Martin, J. M. L.; El-Yazal, J. *J. Phys. Chem.* **1995**, *99*, 13 839.
(20) Burkholder, T. R.; Andrews, L. *J. Chem. Phys.* **1991**, *95*, 8697.
(21) Gaussian 94, Revision B.1. Frisch, M. J.; Trucks, G. W.; Schlegel, H. B.; Gill, P. M. W.; Johnson, B. G.; Robb, M. A.; Cheeseman, J. R.; Keith, T.; Petersson, G. A.; Montgomery, J. A.; Raghavachari, K.; Al-Laham, M. A.; Zakrzewski, V. G.; Ortiz, J. V.; Foresman, J. B.; Cioslowski, J.; Stefanov, B. B.; Nanayakkara, A.; Challacombe, M.; Peng, C. Y.; Ayala, P. Y.; Chen, W.; Wong, M. W.; Andres, J. L.; Replogle, E. S.; Gomperts, R.; Martin, R. L.; Fox, D. J.; Binkley, J. S.; Defrees, D. J.; Baker, J.; Stewart, J. P.; Head-Gordon, M.; Gonzalez, C.; Pople, J. A. Gaussian, Inc., Pittsburgh, PA, 1995.
(22) Becke, A. D. *Phys. Rev. A* **1988**, *38*, 3098. Perdew, J. P. *Phys. Rev. B* **1986**, *33*, 8822.
(23) McLean, A. D.; Chandler, G. S. *J. Chem. Phys.* **1980**, *72*, 5639.
(24) Krishnan, R.; Binkley, J. S.; Seeger, R.; Pople, J. A. *J. Chem. Phys.* **1980**, *72*, 650.
(25) Lanzisera, D. V.; Andrews, L. *J. Am. Chem. Soc.* **1997**, *119*, 6392.
(26) Galland, N.; Hannachi, Y.; Lanzisera, D. V.; Andrews, L. *Chem. Phys.*, to be published.
(27) Tague, T. R., Jr.; Andrews, L. *J. Am. Chem. Soc.* **1994**, *116*, 4970.
(28) Jacox, M. E. *Chem. Phys.* **1975**, *7*, 424.
(29) Shephard, R. A.; Doyle, T. J.; Graham, W. R. M. *J. Chem. Phys.* **1988**, *89*, 2738.
(30) Lanzisera, D. V.; Hassanzadeh, P.; Hannachi, Y.; Andrews, L. *J. Am. Chem. Soc.* **1997**, *119*, 12402.
(31) Heinrich, N.; Koch, W.; Frenking, G.; Schwarz, H. *J. Am. Chem. Soc.* **1986**, *108*, 593.
(32) Wiberg, K. B.; Cheesman, J. R.; Ochterski, J. W.; Frisch, M. J. *J. Am. Chem. Soc.* **1995**, *117*, 6535.
(33) Martin, J. M. L.; Taylor, P. R.; Yustein, J. T.; Burkholder, T. R.; Andrews, L. *J. Chem. Phys.* **1993**, *99*, 12.
(34) Presilla-Marquez, J. D.; Larson, C. W.; Carrick, P. G.; Rittby, C. M. L. *J. Chem. Phys.* **1996**, *105*, 3398.
(35) Smith, D. W.; Andrews, L. *Spectrochim. Acta* **1972**, *28A*, 493.
(36) Herzberg, G. *Infrared and Raman Spectra of Polyatomic Molecules*; D. Van Nostrand, New York, 1945.
(37) Lanzisera, D. V.; Andrews, L. *J. Phys. Chem. A.* **1997**, *101*, 824.
(38) Becher, H. J.; Bramsiepe, F. *Spectrochim. Acta* **1979**, *35A*, 53.